Thermal stimulation temperature is encoded as a firing rate in a *Hydra* nerve ring

Constantine N. Tzouanas[1,4], Soonyoung Kim[2,4], Krishna N. Badhiwala[1], Benjamin W. Avants[2], Jacob T. Robinson[1,2,3*]

1. *Department of Bioengineering, Rice University, 6100 Main Street, Houston, Texas 77005, USA.*
2. *Department of Electrical and Computer Engineering, Rice University, 6100 Main Street, Houston, Texas 77005, USA*
3. *Department of Neuroscience, Baylor College of Medicine, One Baylor Plaza, Houston, Texas 77030, USA*
4. These authors contributed equally.

* To whom correspondence should be addressed: jtrobinson@rice.edu (J.T.R.)

Abstract

Nervous systems are remarkable for supporting stable animal behavior despite dramatic changes to neurons' number and connectivity. An ideal model organism to study this phenomenon would have: 1) dynamic neural architecture 2) transgenic reporters of neural activity, 3) a small, transparent body, and 4) well-defined sensory-motor behaviors. While *Hydra vulgaris* possesses the first three advantages, it currently lacks well-characterized sensory-motor responses. Here, we show the first quantitative measurements of *Hydra*'s behavioral responses to thermal stimulation and associated neural activity. Specifically, we find that *Hydra* elongate and then contract when heated. This behavior is accompanied by synchronous, periodic activity of neurons in the animal's peduncle. We find that the frequency of these neural oscillations is nearly the same even if the number of neurons change by a factor of two. These observations suggest that *Hydra* provides a rich model for studying how animals maintain stable sensory-motor responses within dynamic neural circuit architectures.

One sentence summary: *Here we show that Hydra have a group of thermally responsive neurons that encodes the absolute temperature of a thermal stimulus and that this encoding is independent of the number of neurons in the animal.*

Introduction

With the ability to simultaneously image the activity of nearly every cell in the nervous system, small, transparent invertebrates would be ideal for studying neural plasticity; however, most invertebrates show modest regeneration or lack well-developed transgenic techniques. For instance, even weeks after nerve lesions, *Aplysia* shows incomplete recovery of the number of large axons in nerve cores [1], receptive fields [2], and behaviors like head waving during feeding [3] and tail-elicited siphon-withdrawal reflex [4]. Neurons in the central nervous system of *Drosophila* do not regenerate following axotomies in either whole-brain cultures [5] or in larvae [6]. In *C. elegans*, axons of select neurons can regenerate after being severed [7]; however, growth trajectories are error-prone [8] even

when identical neurons across animals are subjected to similar injury protocols [9]. Exceptional neural plasticity can be found in planarians, which can reform entire organisms [10] from small fragments of tissue, but these animals lack a suite of transgenic tools similar to that of *Drosophila* and *C. elegans* [11].

Hydra vulgaris is unique among invertebrate model organisms in that they are amenable to a variety of transgenic techniques and display significant neural plasticity. For instance, two complete individuals can reform after an organism is cut in half [12], and an entire animal can regenerate from an aggregate of individual cells [13]. The regenerative properties of *Hydra*'s nervous system result from the fact that new neurons continually differentiate from interstitial stem cells in the middle of *Hydra*'s body, displacing existing neurons toward *Hydra*'s extremities. Upon reaching the tentacle or peduncle regions, neurons are shed into the surrounding environment, with all neurons being replaced every 20 days [14]. Neurons' connectivity and gene expression profiles vary over time as they follow this trajectory through the body, making it possible to study how new neurons integrate into existing circuits and how neurons regenerate following injury.

The small size and genetic tractability of *Hydra* provide additional advantages. As a millimeter-scale invertebrate, an entire *Hydra* can be imaged at single-cell resolution [15]. Furthermore, the ability to generate transgenic lines by embryo injection [16] has enabled functional calcium imaging in neurons [15] and muscles [17]. In addition, there is hope for cell-type specific promoters based on single-cell transcriptomic analysis of *Hydra* that has revealed twelve neuronal subtypes, each expressing distinct sets of biomarkers linked to neuronal development and function [18].

Given *Hydra's* potential as a model for neural plasticity, it is critical to establish behavioral assays that indicate if and when neural circuits have regained their ability to regulate behavior. While *Hydra* has been studied for over 300 years, we lack quantitative characterization of behaviors like sensory-motor responses. This knowledge gap is due, in part, to difficulty in tracking sufficient numbers of these slowly moving, tiny, and nearly transparent animals. Observations of behavior in individual or small numbers of animals date back to the 1700's [19] describing responses to light [20], chemicals [21], and temperature [22]–[24]. More recently, behavioral motifs have been identified in freely moving animals.

Several experiments suggest that *Hydra* can sense temperature, but there has yet to be an unambiguous report of *Hydra's* behavioral response to an acute thermal stimulus. Mast showed that when touched by heated objects, *Hydra* responds by bending toward the object. Schroeder and Callaghan reported the highest and lowest temperatures in which *Hydra oligactis* and *Hydra pseudoligactis* could survive. Bosch et al. demonstrated that exposing *Hydra attenuata (vulgaris)* to moderately elevated temperatures (30°C for two hours) increases their ability to survive culture at high temperatures (34°C for four days) that would otherwise be lethal. While these experiments show that *Hydra* viability depends on the ambient temperature, they do not reveal the specific sensory-motor response to an acute thermal stimulus. Observation of the animal's reaction to contact with a heated object (as in the study by Mast) cannot distinguish between a mechanical or thermal response.

Here we characterize *Hydra's* behavioral and neural response to thermal stimulation by using a microfluidic device that can deliver rapid and precise thermal stimuli without the confound of mechanical stimulation. The multi-layer microfluidic device we designed allows us to rapidly change the temperature of a flow layer that is separate from the *Hydra*'s behavioral chamber (Fig. 1). In this way, changes in temperature do not elicit mechanically-evoked responses. Using this technique, we find that *Hydra* elongates after the onset of positive thermal stimulation, followed by a contraction lasting for the stimulus duration. Synchronous with body movements, we find temperature-dependent oscillatory neural activity within a ring of neurons in *Hydra*'s peduncle. The frequency of this oscillation decreases for negative thermal stimulation and increases for positive thermal stimulation. Finally, we show that the frequency of the neural oscillation depends primarily on the absolute temperature of the thermal stimuli. Importantly, we find that these frequencies are nearly unchanged if animals are cultured at different temperatures or if animals have two-fold differences in the number of neurons.

Results

Microfluidic device enables thermal stimulation and whole-body imaging of *Hydra vulgaris*

Because *Hydra* are known to be sensitive to mechanical stimulation (e.g., touch and changes in fluid flow [25], [26]), we designed a two-layer microfluidic device to deliver thermal stimuli without mechanical confounds: a *Hydra* immobilization chamber fabricated above a flow layer with multiple inlet ports (Fig. 1a, see methods). By connecting the flow layer's inlet ports to in-line heaters at different temperature setpoints, we can provide rapid and precise thermal stimulation by switching fluid flow through the different inlet ports – a process that we automate using microcontrollers (see methods). In our experiments, one inlet (i in Fig. 1a) provides fluid that is maintained at *Hydra*'s culture temperature to serve as a control. The second inlet provides fluid that is maintained at a stimulus temperature ranging from 9-36°C. To validate our ability to rapidly and repeatedly modulate the temperature of the *Hydra* immobilization chamber, we measured the temperature of the device glass with an IR camera (Fig. 1b-c). We found that we could switch between temperature setpoints in approximately one second, and that the temperature set points were repeatable to within a standard deviation of 0.5^{o}C through at least 3 stimulation cycles.

We then confirmed that our thermal stimulation method did not produce mechanical stimulation artifacts. From measurements of *Hydra*'s behavioral and neural activity while switching between two fluid sources maintained at *Hydra*'s culture temperature, we observed no statistically significant changes to *Hydra*'s body length as compared to experiments with no fluid flow. These results indicate that changes in fluid flow do not drive behavioral or neural responses or activate mechanosensory pathways. On the other hand, when we switch between fluids at different temperatures, we find consistent behavioral and neural responses. For example, when we switch between 18°C and 30°C, we observe animal elongation (Fig. 2) and an increase in neural activity (Fig. 3). These results demonstrate that we can both stimulate and measure sensory-motor responses in *Hydra* using this thermal stimulation protocol.

Positive thermal stimulation drives sequential elongation and contraction in *Hydra vulgaris*

With the ability to apply rapid and precise thermal stimuli while imaging entire *Hydra*, we characterized *Hydra*'s behavioral responses to thermal stimulation. To avoid synchronizing the stimuli with natural rhythmic behavior [26], [27] or entraining a periodic response, we applied the thermal stimuli for a period of 60 seconds and randomized the time interval between successive stimuli (Fig. 2a). To quantify changes in *Hydra*'s posture, we applied DeepLabCut [28] to automate labeling of *Hydra*'s body width and length (Fig. 2b).

We found *Hydra* respond to a rapid change in temperature (18°C to 30°C over approximately 1 s) by first elongating, and then contracting. The peak body length occurs approximately 20 seconds after the stimulus onset (Fig. 2c-d). When we switched the flow layer source between two reservoirs at the 18°C culture temperature we observed no a significant change in body width or length as compared to

measurements with no flow through the lower chamber (Fig. 2d). These data support the conclusion that the elongation and subsequent contraction we observed during thermal stimulation is indeed driven by *Hydra* thermosensation.

Spike rate of periodic neural activity in the *Hydra vulgaris* peduncle is temperature sensitive.

Using calcium imaging we also found that a select group of neurons shows an increase in firing rate following a rapid change in temperature. From fluorescent imaging of *Hydra* that express GCaMP6s in the neurons, we found a cluster of neurons in *Hydra*'s peduncle that exhibited synchronous periodic activity during thermal stimulation (Fig. 3b). We will refer to these neurons as temperature responsive (TR) neurons. The firing rate of these TR neurons during thermal stimulation is significantly higher than in control experiments where we switched the flow between two reservoirs that were both at the 18°C culture temperature (Fig. 3c-e). We found no statistically significant difference between the firing rates in these control animals, and the firing rate in animals with no changes to the flow in the lower microfluidic layer, suggesting that the increase in neural activity observed during thermal stimulation is indeed driven by the rapid change in temperature and not mechanical confounds related to changing flow rates in the lower microfluidic layer.

We also found that the firing rate of the TR neurons during thermal stimulation depends primarily on the absolute temperature of the thermal stimuli and not on the relative increase in temperature. When we cultured *Hydra* at an elevated temperature of 25°C (compared to the common 18°C) we found nearly the same trend in firing rate as a function of stimulation temperature as animals cultured at 18°C (Fig. 3f). At higher stimulation temperatures (30°C and 36°C) a paired T-test shows statistically significant differences between animals cultured at 18°C and 25°C temperatures, but the effect size (Cohen's d) of changing the culture temperature by 7°C is much smaller than the effect size of changing the stimulation temperature by 6°C (between 30°C and 36°C). These results support the conclusion that TR neurons do not encode information about relative changes in temperature, but rather that they primarily encode the absolute temperature of a thermal stimulus.

Hydra vulgaris' neural response to thermal stimulation is robust against two-fold changes in neuron count

Having identified that TR neurons encode the absolute temperature of a thermal stimulus, we asked if this encoding is maintained even if animals have significantly different numbers of neurons. To answer this question, we first determined that the number of neurons in *Hydra* is linearly related to the size of the animal. Using longitudinal fluorescence imaging of *Hydra* over two weeks of starvation or regular feedings, we found that the number of interstitial cells (comprising neurons and nematocysts) scaled with *Hydra*'s body volume, consistent with prior reports of the density of neurons as a function of animal size [29], [30] (Fig. 4a-c).

We found that the TR neuron response to thermal stimuli was nearly identical in animals with a two-fold difference in the number of neurons suggesting that *Hydra* maintain stable encoding of thermal

stimuli despite significant differences in the size of their neural circuits. To compare animals with different sizes, we separated animals into “large” and “small” cohorts based on body size. Based on the differences in body size and our measured relationship between body size and number of neurons, we estimate that the difference in neuron count between these groups is approximately two-fold (Fig. 4d-e). When we measured the spike rates during thermal stimulation, we found a nearly identical temperature dependence for both small and large animals (Fig. 4f). At some temperatures we did find statistically significant differences between the thermal response of the “small” and “large” animals (at 12°C and 24°C, Fig. 4f), but the effect size (Cohen’s d) is small compared to the effect size of changing the temperature by 4-5°C. Thus, despite remodeling their nervous system to account for a two-fold increase or decrease in the numbers of neurons, *Hydra* are able to consistently encode the temperature of a thermal stimulus.

Discussion

Unlike many invertebrate model systems like *C. elegans* and *Drosophila* that have stereotyped neural architecture with well-defined numbers of neurons, *Hydra*'s highly plastic nervous system allows us to study how behaviors like sensory-motor responses are maintained as neural circuits remodel and incorporate new neurons. The two-layer microfluidic device shown here is one way to study this process because it allows us to simultaneously image neural activity and behavior while we deliver thermal stimuli. Using this technology, we were able to characterize *Hydra's* response to a rapid change in temperature. We found that during a thermal stimulation the animal first elongates and then contracts, with the peak body length occurring approximately 20 seconds after the stimulus onset. This behavioral response to a thermal stimulus is accompanied by synchronous periodic activity in a group of neurons near the animal's aboral end that we refer to as the TR neurons. The frequency of TR neuron activity depends on the absolute temperature of the thermal stimulus, and this encoding is maintained even if the number of neurons in the animal changes by a factor of two.

One remaining question is the identity of the TR neurons. Their location near the animal's foot suggests that they may be the contraction burst (CB) neurons that are associated with animal contractions [15], but more work is needed to determine if TR neurons and CB neurons are a completely overlapping neuronal subtype. This could be answered using cell type specific promoters or other cell-type labeling strategies that can be developed based on recent single-cell transcriptomic data [18].

Another question is how the TR neurons maintain their thermal response properties in circuits of different sizes. It is possible that *Hydra* have homeostatic mechanisms to maintain a neural circuit architecture that has the same thermal response even as neurons are added and removed. Alternatively, the TR response may be a cellular property that is independent of the circuit size and architecture. The answer to this question could be elucidated by single cell electrophysiology or by blocking cell-to-cell signaling in this circuit. These methods do not yet exist for *Hydra*, but would be powerful methods to better understand this neural circuit.

By studying sensory-motor transformations like this thermal response we may also learn about fundamental properties of neural circuits that are common to many species. For example, the TR neurons shows characteristics of a neural oscillator, which is a common motif across phylogeny. Because *Hydra* is a member of the sister phylum to all animals with bilateral symmetry (bilateria), we may be able to compare neural oscillators in animals from different phyla. In this way we may be able to learn conserved principles of neural circuits that appeared early in our evolutionary history.

Overall, the ability to study neural and behavioral responses to thermal stimulation in an animal with a high-rate of neural regeneration and is amenable to cellular-resolution fluorescent imaging offers many advantages for uncovering how neural circuits remodel without compromising their function.

Materials and Methods

Microfluidic device fabrication:

All microfluidic devices were fabricated using polydimethylsiloxane (PDMS) (Sylgard 184). The thermal stimulation chip is a two-layer device: bottom stimulus flow channels and a top *Hydra* immobilization chamber, separated by a glass coverslip. By separating *Hydra* from fluid flow, the animal can be rapidly heated/cooled (by flowing water at controlled temperatures through the bottom stimulus flow channels) without undesired mechanical stimulation from high flow rates (avoided due to the glass coverslip separation). To construct the double layer chip, we first fabricated the top immobilization layer by molding PDMS from a master mold adapted from a 2 mm diameter x 100 μm tall chemical perfusion chip (designed as previously described) [31]. Briefly, a circular observation chamber designed specifically for *Hydra* was patterned using soft lithography on a silicon substrate, and a ~5mm thick layer of PDMS was molded from this master mold. After punching holes for the inlet and outlet ports with a 1.5mm diameter biopsy punch, the immobilization layer was O_2 plasma bonded to a 12mm diameter glass coverslip.

This top immobilization chip was then placed with glass coverslip side facing down directly on the center of the master mold for the flow layer. Uncured PDMS was poured into the flow layer mold surrounding the immobilization chamber, taking care not to clog the ports in the immobilization layer. The master mold for the flow layer (adapted from Duret et al [32]) was 3D-printed with 1mm tall channels (Form 2, Flexible Resin, Formlabs). After curing the PDMS for the bottom flow layer (thereby embedding the immobilization chamber), holes were punched for inlet/outlet access for the flow layer. Finally, this double layer microfluidic chip was O_2 plasma bonded to a 500 μm fused silica wafer (University Wafer).

After unloading *Hydra* from the device at the end of a trial (see “Loading and unloading *Hydra*”), both layers of the microfluidic device were rinsed with *Hydra* media (media adapted from the laboratory of Robert Steele), sonicated in *Hydra* media for at least 10 minutes, and soaked at room temperature in *Hydra* media. Such cleaning allowed for devices to be reused across multiple days of trials.

Hydra strains and maintenance:

All trials were conducted on transgenic lines with neuronal expression of GCaMP6s, developed with embryo microinjections by Christopher Dupre in the laboratory of Rafael Yuste. *Hydra* were cultured using the protocol adapted from the laboratory of Robert Steele (UC Irvine). *Hydra* were raised at either 18ºC or 25ºC in incubators, both with 12:12 hours light:dark cycle. Animals were fed freshly hatched artemia nauplii three times a week and cleaned after approximately 4 hours with *Hydra* media. All animals used in trials were starved for a day prior to thermal stimulation experiments and were not re-used.

Loading and unloading *Hydra*:

Hydra were loaded into the inlet port of Hydra enclosure using a 10 mL syringe with attached tygon tubing. *Hydra* were then pulled a couple of centimeters into the tygon tubing before the tubing was inserted into the inlet port of the microfluidic device. By applying gentle pressure and gently pulsing on the plunger of the syringe, *Hydra* could be successfully loaded into the immobilization chamber without damage from mechanical shear. After the experiments, *Hydra* was removed from the device by applying pressure on the plunger of a tygon tubing-attached syringe and flushing the organism out the outlet port.

Thermal stimulation assay:

After loading *Hydra*, two programmable syringe pumps (New Era NE-500) controlled by an Arduino Mega ADK were used to drive the flow of deionized water at a rate of 6 mL/min through two inlet ports of the thermal stimulation device. The third inlet port was connected to an additional syringe (useful for removing air bubbles when initially filling the bottom stimulus flow channels prior to the start of a trial), and the device outlet port was connected to a water collection container. Fluid flow from the two pumps was heated/cooled using two in-line heaters (SC-20, Warner Instruments) regulated by a Dual Channel Bipolar Temperature Controller (CL-200A, Warner Instruments). One in-line heater supplied *Hydra*'s culture temperature during control periods (i.e. 18°C or 25°C), while the other heater supplied the desired stimulus temperature of a given trial (i.e. 9°C, 12°C, 18°C, 24°C, 25°C, 30°C, or 36°C). To compensate for heat exchange between water flowing through inlet tubing and the environment, a FLIR ONE thermal camera was used to calibrate the relationship between in-line heater temperature settings and actual temperatures of the thermal stimulation device.

Each thermal stimulation trial began with two minutes at *Hydra*'s culture temperature. Subsequently, the trial alternated between stimulus periods (single temperature for a given trial; 9°C, 12°C, 18°C, 24°C, 25°C, 30°C, or 36°C) and control periods (based on *Hydra*'s culture temperature; 18°C or 25°C). Stimulus periods always lasted for 60 seconds, while control periods varied in length between 30 and 90 seconds in 15 second increments, to help distinguish between stimulus-evoked responses and spontaneous activity. The lengths of control periods were randomly ordered and averaged to 60 seconds over the course of a trial. For a visual representation of thermal stimulation protocols, see Fig. 3a. The timing of transitions between stimulus and control periods were recorded through the Arduino's Serial Monitor (57600 baud rate) and used to determine portions of recordings corresponding to stimulus and control periods. For experiments on size comparison of *Hydra* cultured at 18°C, 3 large and 3 small animals for each temperature (9°C, 12°C, 18°C, 24°C, 30°C, and 36°C), 36 animals in total were used over the course of 15 days. For *Hydra* cultured at 25°C, 3 animals were used at 18°C, and 4 animals at 25°C, 30°C, and 36°C over the course of 7 days.

Fluorescence imaging was conducted on a Nikon SMZ18 stereomicroscope with a SHR Plan Apo 2x objective (0.3 NA) and Andor Zyla 4.2 (16 fps, 3x3 image binning). Excitation was provided by a X-Cite Xylis XT720L at 50% intensity through a Chroma EGFP filter cube (catalog no. 49002).

Longitudinal imaging of the entire nervous system

Transgenic *Hydra vulgaris* AEP expressing GFP (green fluorescent protein) in their interstitial cell lineage were used to investigate how the number of neurons varies with animal size and nutrient availability. Animals with large body size (>2 mm long) at the beginning of the study were starved for the duration of the experiment. A control group of animals with small body size (< 1mm) at the beginning of the study were fed with an excess of freshly hatched artemia nauplii three times a week. Size of the animal was defined as the length of the animal in a relaxed state (between fully contracted and fully elongated). *Hydra* media was replaced daily for all animals.

Volumetric imaging was performed using a confocal microscope (Nikon TI Eclipse) with animals immobilized in chemical perfusion microfluidic chips (see Badhiwala et al. [31]) and chemically paralyzed with 1:5000 linalool. Animals were imaged three times a week (one day after the control animals were fed) over two weeks. All images were acquired with a 10x DIC objective. The majority of the images were acquired with 1024 x 1024 pixels (x, y) resolution and 5 mm z-resolution. A lower resolution of 512 x 512 pixels and 10 mm z-resolution were used in a few cases to speed up volumetric imaging where micromotions of the animals could not be completely eliminated with chemical anesthetic (becoming increasingly important with animals starved for extended periods of time).

To quantify the total number of neurons, a maximum intensity projection image was generated from the z-stacks. After binarizing the resultant image with a user-defined threshold, individual regions (or neurons) were summed to determine the total number of neurons. However, due to anatomical overlap of multiple neurons in high-density regions such as the peduncle, future work will focus on developing transgenic animals that express fluorescent reporters in the nuclei of specific neural cell types, rather than in the cytosol of interstitial cell derived lineages (as in the animals used here).

To quantify the body size during an experiment, we binarized the maximum intensity projection image with a lower threshold than above. Filling holes in the binarized image produced the binary mask for the whole animal. Body size was calculated as the area of this binary region, and body volume was body size times the thickness of the immobilization chamber (160 μm).

The duration of the experiment was kept under two weeks, as well-fed animals can reproduce asexually by budding every 3-4 days. In fact, one of the animals in well-fed group began forming a bud on day 10 of the experiment. Additionally, as animals are starved, they become smaller and more transparent, making them difficult to handle. In our starved group, we 'lost' one of the animals on day 15 as it was either too transparent or had shrunk considerably to not be discerned from the plate.

Behavioral analysis

DeepLabCut [28] along with custom MATLAB code was used to quantify *Hydra*'s behavioral responses to thermal stimuli. 20 frames per video were extracted for manual tracking according to k-means clustering on DeepLabCut. *Hydra* in each frame then was manually annotated with the locations of basal disc, left side, center, and right side of the body, and hypostome. Two corners of the immobilization chamber were additionally annotated, providing a known distance (2 mm) to convert pixel

measurements to micrometer measurements. The annotated dataset was used as training data for DeepLabCut. After evaluating the model, the videos were analyzed using the trained model which yielded the coordinates of the seven points listed above for every frame (total of 14,600 frames) for every video, along with annotated videos. With the coordinates obtained from DeepLabCut annotations, body width was calculated as the sum of the distance from the left side to the middle of the body and the distance from the middle to the right side of the body, and body length was calculated as the sum of the distance from the hypostome to the middle of the body and the distance from the middle of the body to the basal disc (Fig. 2b, bottom panel) with a custom MATLAB code.

Analysis of neural activity in the peduncle of Hydra

To determine the timing and frequency of spikes in *Hydra*'s peduncle oscillator, fluorescence microscopy recordings from thermal stimulation trials of neuronal GCaMP6s *Hydra* (see "Thermal Stimulation Assay") were processed in Fiji (ImageJ) and in MATLAB. For each frame of the recording, Fiji was used to calculate the average intensity of a ROI encompassing *Hydra*'s peduncle and aboral regions (same ROI for the entire recording). In MATLAB, this intensity trace was smoothed (5 data point span), and the built-in findpeaks function was used to determine spike locations based on their prominence in the intensity traces. Spurious spikes (e.g. from measurement noise) were eliminated by additionally testing that each identified peak was the only local maximum exceeding a threshold prominence value within a narrow window of the peak.

Raster plots were then directly produced from the times of peduncle oscillator spikes during each stimulus period and the surrounding 30 seconds at culture temperature. Peristimulus time histograms were calculated by counting the number of spikes across all stimulus periods at a given stimulation temperature in a 10-second sliding window, then normalizing by the number of stimulus periods and the length of the window. Instantaneous spike rates for a given thermal stimulus temperature were calculated as the inverse of interspike intervals during stimulus periods.

Acknowledgements

We would like to thank Dr. Christophe Dupre and Dr. Rafael Yuste (Columbia University), Dr. Celina Juliano (UC Davis) and Dr. Rob Steele (UC Irvine) for sharing transgenic *Hydra* lines.
K.N.B. is funded by training fellowships from the Keck Center of the Gulf Coast Consortia on the NSF Integrative Graduate Education and Research Traineeship (IGERT): Neuroengineering from Cells to Systems 1250104.

Author Contributions

C.N.T. and S.K. performed and analyzed *Hydra* thermal stimulation experiments. K.N.B. performed and analyzed longitudinal imaging experiments on *Hydra*'s number of neurons as a function of body size. C.N.T., K.N.B., and B.W.A. designed, prototyped, and fabricated the microfluidic device. C.N.T.,

S.K., and B.W.A. implemented microcontroller automation of thermal stimulation experiments. C.N.T., S.K., K.N.B., and J.T.R. co-wrote the paper. All authors read and commented on the manuscript.

Conflict of Interest

Authors declare no conflict of interest.

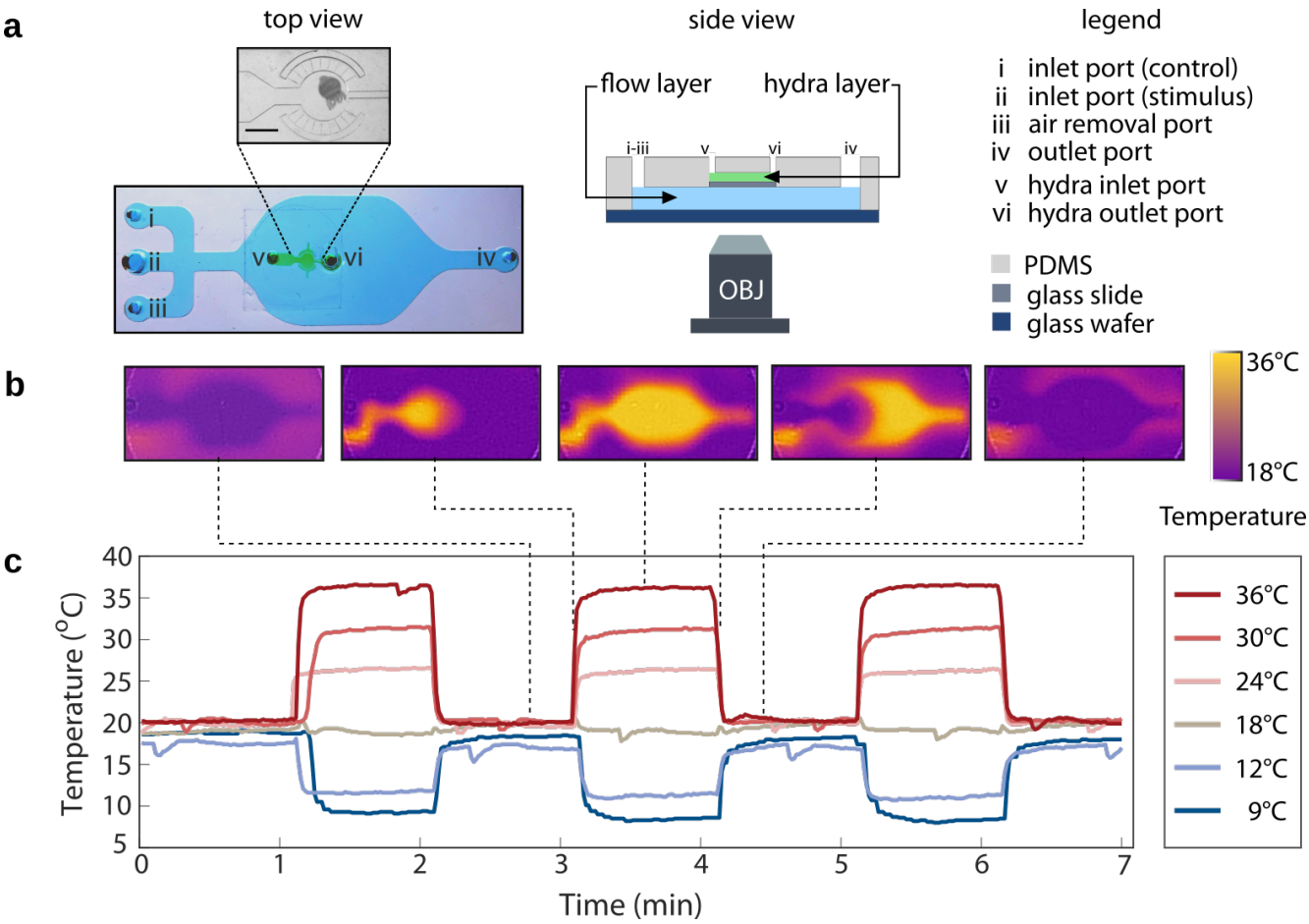

Fig. 1 Characterization and validation of two-layer microfluidic device for thermal stimulation of *Hydra vulgaris*. a (left) Photograph of microfluidic device with blue dye in flow layer and green dye in *Hydra* chamber. Scale bar = 1 mm. (middle) Schematic of cross-section of the device. (right) legend for left and middle panel. **b** Infrared image showing temperature of the flow layer before (leftmost), the start of (second leftmost), during (center), end of (second rightmost), and after (rightmost) thermal stimulation. **c** Time course of thermal stimulation at temperatures above and below *Hydra*'s baseline culture temperature of 18°C.

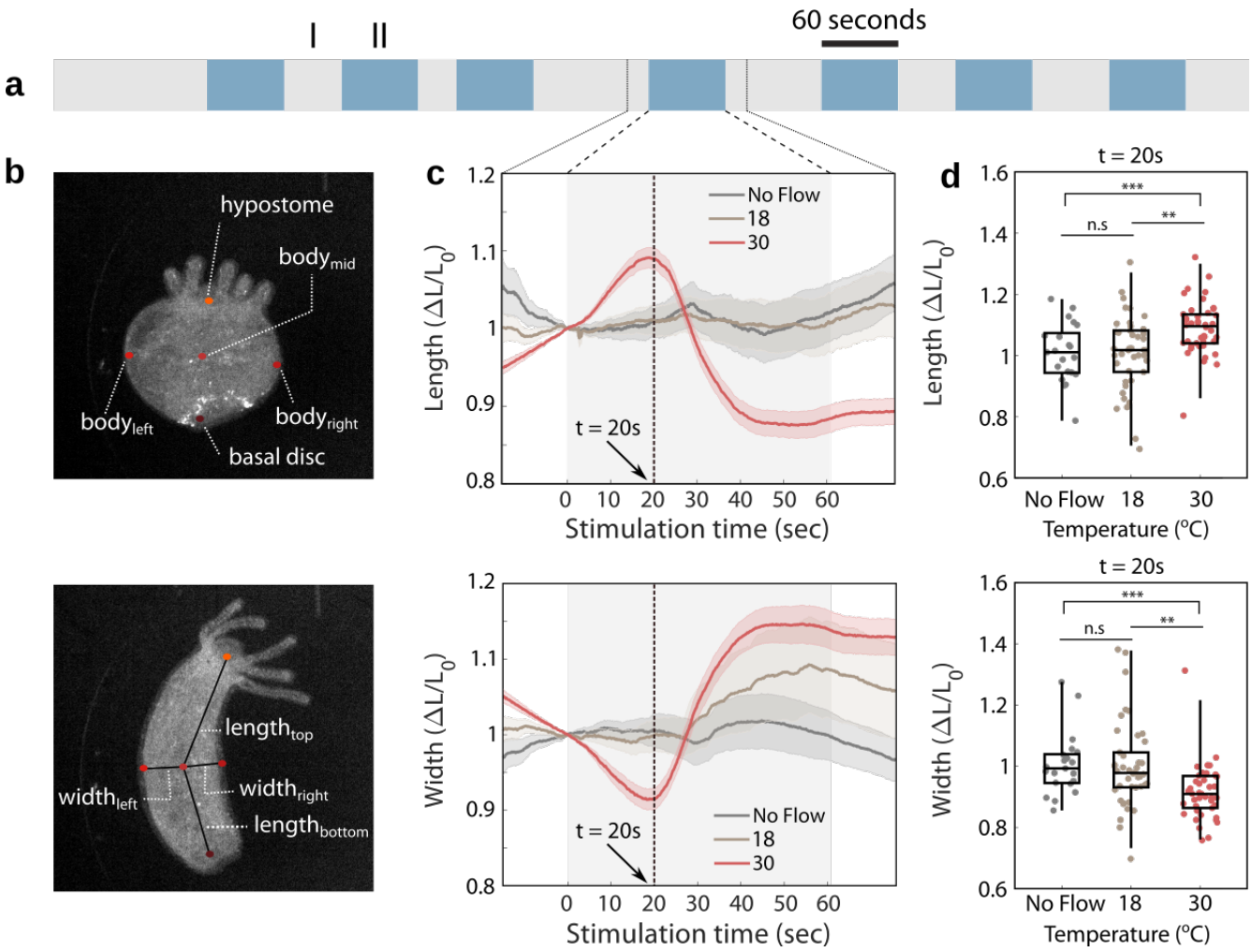

Fig. 2 *Hydra*'s body length initially increases and width initially decreases when stimulated at 30°C. a Schematic of a representative thermal stimulation protocol. Gray regions (I) indicate non-stimulus periods at *Hydra*'s culture temperature lasting between 30 and 90 seconds, and blue-colored regions (II) indicate stimulus periods at designated temperatures for 60 seconds. **b** Representative labeled frame from DeepLabCut, annotated. Top panel describes which body points were annotated, and bottom panel shows how the length and width of the animals are determined. **c** Average length and width of *Hydra* calculated for stimulation periods and time-aligned to stimuli, with 15 seconds before and after stimulation periods. Shaded error bars correspond to standard error. **d** The change in length (top panel) and width (bottom panel) at 20 seconds after onset of stimulation, for each stimulus period (t = 20s). N=3 *Hydra* for No Flow, N=6 *Hydra* for 18oC and 30oC. (n.s = not significant, ** p<0.001, *** p<0.0001, unpaired t-test).

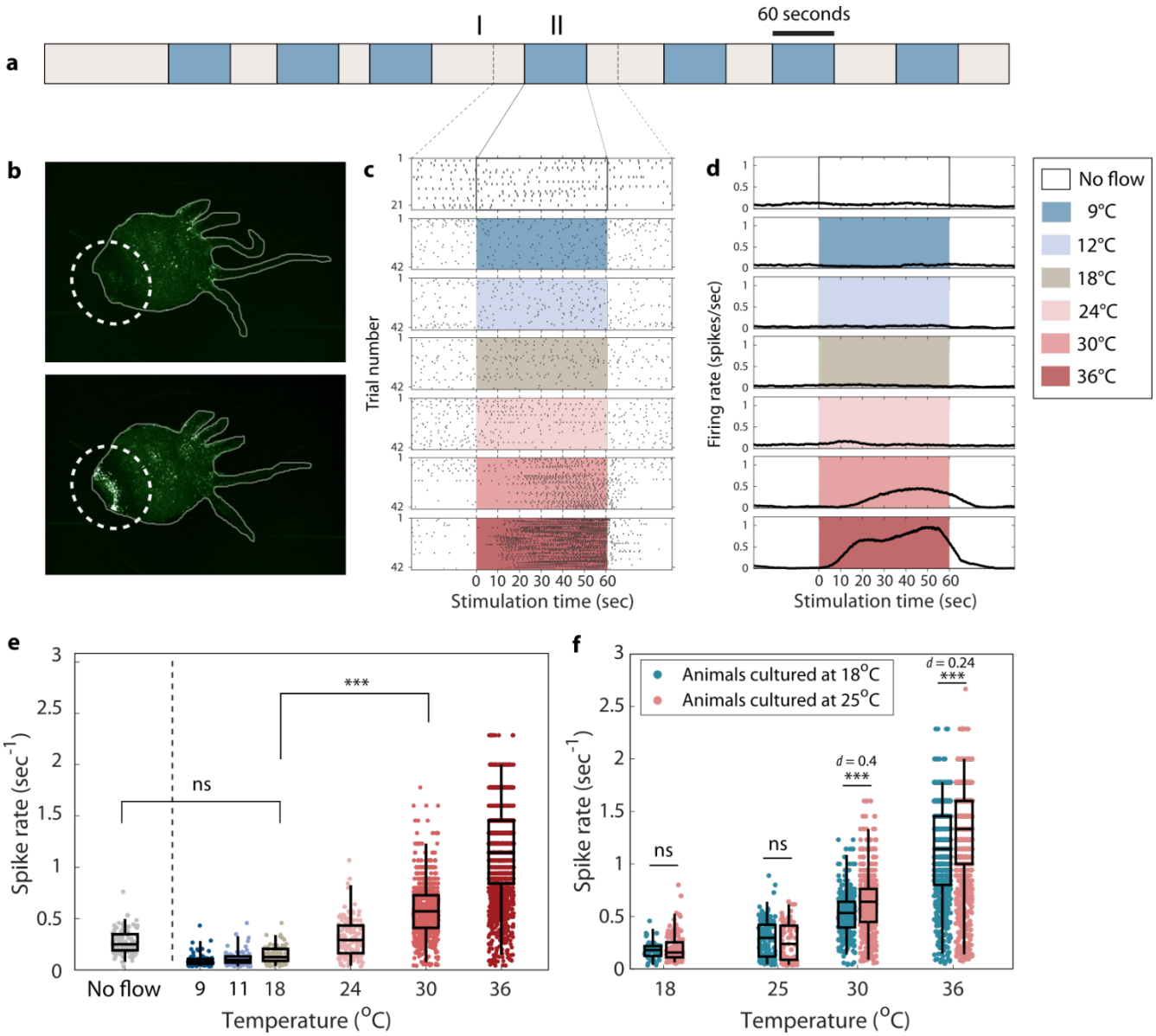

Fig. 3 Thermal stimulation modulates the synchronous neural activity in the peduncle of *Hydra vulgaris* **a** Schematic of a representative thermal stimulation protocol. Gray regions (I) indicate non-stimulus periods at *Hydra*'s culture temperature lasting between 30 and 90 seconds, and blue-colored regions (II) indicate stimulus periods at designated temperatures for 60 seconds. **b** Images of *Hydra* without synchronous neural firing (top) and during firing (bottom) in the peduncle (white circle). **c** Raster plot of synchronous firing events in peduncle in **b**. One black vertical line indicates one synchronous firing event. Each row represents the raster plot of spikes time-aligned with one stimulation (boxed regions) with 30 seconds before and after stimulation (white non-boxed region). **d** Peristimulus time histogram of **c** which was calculated with a 10 second sliding window. **e** Spike rates from large and small *Hydra*, all cultured at 18°C. N=3 large animals; N=3 small animals. (ns = not significant, *** p<0.00001, Kruskal-Wallis test with post hoc Bonferroni correction). **f** Spike rates from Hydra cultured at 18°C and

25°C. X-axis notes the stimulation temperatures. N=3 for all animals. (ns = not significant, *** $p<0.00001$, unpaired t-test. d = Effect size using Cohen's d method.)

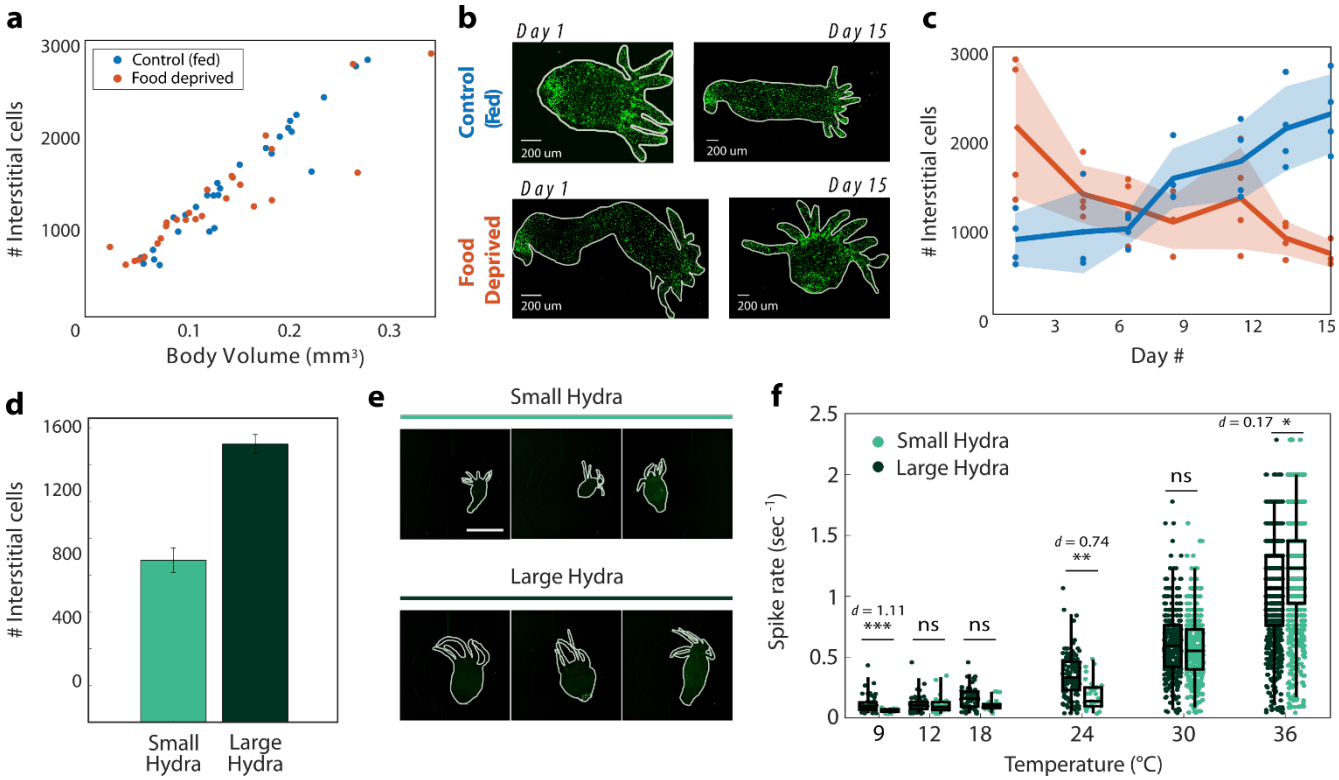

Fig. 4 Frequency of thermal response neurons does not depend on number of neurons in *Hydra*. **a** Number of interstitial cells (including neurons and nematocysts) as a function of animal size. **b** Fluorescent image of Hydra at days 1 and 15 for both control and food deprived group (pseudo colored). **c** Change in the number of interstitial cells over the time course of 15 days. **d** Estimated number of interstitial cells from measurements in **a**. **e** Three representative *Hydra* from small and large groups (pseudo colored) Scale bar = 500 μm. **f** Spike rates from large (N=3) and small (N=3) *Hydra*, all cultured at 18°C. (ns = not significant, * $p<0.05$, ** $p<0.001$, *** $p<0.00001$, unpaired t-test. d = Effect size using Cohen's d method.)

References

[1] M. L. Scott, S. C. Danzer, C. K. Govind, and M. D. Kirk, “Morphological correlates of neural regeneration in the feeding system of Aplysia californica after central nervous system lesions,” *J. Comp. Neurol.*, vol. 387, no. 2, pp. 279–290, Oct. 1997.

[2] M. F. Dulin, I. Steffensen, C. E. Morris, and E. T. Walters, “Recovery of function, peripheral sensitization and sensory neurone activation by novel pathways following axonal injury in Aplysia californica.,” *J. Exp. Biol.*, vol. 198, no. 10, pp. 2055 LP – 2066, Oct. 1995.

[3] I. Kupfermann, “Dissociation of the appetitive and consummatory phases of feeding behavior in Aplysia: a lesion study,” *Behav. Biol.*, vol. 10, no. 1, pp. 89–97, Jan. 1974.

[4] F. Noel, W. N. Frost, L. M. Tian, M. A. Colicos, and P. K. Dash, “Recovery of tail-elicited siphon-withdrawal reflex following unilateral axonal injury is associated with ipsi- and contralateral changes in gene expression in Aplysia californica,” *J. Neurosci.*, vol. 15, no. 10, pp. 6926 LP – 6938, Oct. 1995.

[5] D. Ayaz *et al.*, “Axonal Injury and Regeneration in the Adult Brain of Drosophila,” *J. Neurosci.*, vol. 28, no. 23, pp. 6010 LP – 6021, Jun. 2008.

[6] Y. Song, K. M. Ori-McKenney, Y. Zheng, C. Han, L. Y. Jan, and Y. N. Jan, “Regeneration of Drosophila sensory neuron axons and dendrites is regulated by the Akt pathway involving Pten and microRNA bantam,” *Genes Dev.*, vol. 26, no. 14, pp. 1612–1625, Jul. 2012.

[7] M. F. Yanik, H. Cinar, H. N. Cinar, A. D. Chisholm, Y. Jin, and A. Ben-Yakar, “Functional regeneration after laser axotomy,” *Nature*, vol. 432, no. 7019, p. 822, 2004.

[8] Z. Wu, A. Ghosh-Roy, M. F. Yanik, J. Z. Zhang, Y. Jin, and A. D. Chisholm, “Caenorhabditis elegans neuronal regeneration is influenced by life stage, ephrin signaling, and synaptic branching,” *Proc. Natl. Acad. Sci.*, vol. 104, no. 38, pp. 15132–15137, Sep. 2007.

[9] M. Hammarlund and Y. Jin, “Axon regeneration in C. elegans,” *Curr. Opin. Neurobiol.*, vol. 27, pp. 199–207, Aug. 2014.

[10] P. W. Reddien, “The Cellular and Molecular Basis for Planarian Regeneration,” *Cell*, vol. 175, no. 2, pp. 327–345, Oct. 2018.

[11] M. L. Scimone, L. E. Cote, and P. W. Reddien, “Orthogonal muscle fibres have different instructive roles in planarian regeneration,” *Nature*, vol. 551, p. 623, Nov. 2017.

[12] R. L. Roudabush, “Present Status of Longitudinal Division in Hydra,” *Biol. Bull.*, vol. 66, no. 3, pp. 326–329, 1934.

[13] U. Technau *et al.*, “Parameters of self-organization in Hydra aggregates,” *Proc. Natl. Acad. Sci.*, vol. 97, no. 22, pp. 12127 LP – 12131, Oct. 2000.

[14] R. D. Campbell, “Tissue dynamics of steady state growth in Hydra littoralis. II. Patterns of tissue movement,” *J. Morphol.*, vol. 121, no. 1, pp. 19–28, Jan. 1967.

[15] C. Dupre *et al.*, “Non-overlapping Neural Networks in Hydra vulgaris,” *Curr. Biol.*, vol. 27, no. 8, pp. 1085–1097, 2017.

[16] C. E. AU - Juliano, H. AU - Lin, and R. E. AU - Steele, “Generation of Transgenic Hydra by Embryo Microinjection,” *JoVE*, no. 91, p. e51888, 2014.

[17] J. R. Szymanski and R. Yuste, “Mapping the Whole-Body Muscle Activity of Hydra vulgaris,” *Curr. Biol.*, vol. 29, no. 11, pp. 1807-1817.e3, Jun. 2019.

[18] S. Siebert *et al.*, “Stem cell differentiation trajectories in Hydra resolved at single-cell resolution,” *Science (80-.).*, vol. 365, no. 6451, p. eaav9314, Jul. 2019.

[19] R. D. CAMPBELL, “Taxonomy of the European Hydra (Cnidaria: Hydrozoa): a re-examination of its history with emphasis on the species H. vulgaris Pallas, H. attenuata Pallas and H. circumcincta Schulze,” *Zool. J. Linn. Soc.*, vol. 95, no. 3, pp. 219–244, May 2008.

[20] L. M. PASSANO and C. B. MCCULLOUGH, “Pacemaker Hierarchies Controlling the Behaviour of Hydras,” *Nature*, vol. 199, no. 4899, pp. 1174–1175, 1963.

[21] W. A. Kepner and D. L. Hopkins, “Reactions of Hydra to chloretone,” *J. Exp. Zool.*, vol. 38, no. 4, pp. 437–448, Jan. 1924.

[22] L. A. Schroeder and W. M. Callaghan, “Thermal tolerance and acclimation of two species of Hydra1,” *Limnol. Oceanogr.*, vol. 26, no. 4, pp. 690–696, Jul. 1981.

[23] S. O. Mast, “REACTIONS TO TEMPERATURE CHANGES IN SPIRILLUM, HYDRA, AND FRESH-WATER PLANARIANS,” *Am. J. Physiol. Content*, vol. 10, no. 4, pp. 165–190, Dec. 1903.

[24] T. C. Bosch, S. M. Krylow, H. R. Bode, and R. E. Steele, “Thermotolerance and synthesis of heat shock proteins: these responses are present in Hydra attenuata but absent in Hydra oligactis,” *Proc. Natl. Acad. Sci. U. S. A.*, vol. 85, no. 21, pp. 7927–7931, Nov. 1988.

[25] N. B. Rushforth, A. L. Burnett, and R. Maynard, “Behavior in Hydra: Contraction Responses of Hydra pirardi to Mechanical and Light Stimuli,” *Science (80-.).*, vol. 139, no. 3556, pp. 760 LP – 761, Feb. 1963.

[26] L. M. PASSANO and C. B. McCULLOUGH, “Co-Ordinating Systems and Behaviour In Hydra: I. Pacemaker System of the Periodic Contractions,” *J. Exp. Biol.*, vol. 41, no. 3, pp. 643 LP – 664, Sep. 1964.

[27] N. B. RUSHFORTH, “BEHAVIORAL AND ELECTROPHYSIOLOGICAL STUDIES OF HYDRA. I. ANALYSIS OF CONTRACTION PULSE PATTERNS,” *Biol. Bull.*, vol. 140, no. 2, pp. 255–273, Apr. 1971.

[28] T. Nath, A. Mathis, A. C. Chen, A. Patel, M. Bethge, and M. W. Mathis, “Using DeepLabCut for 3D markerless pose estimation across species and behaviors,” *Nat. Protoc.*, vol. 14, no. 7, pp. 2152–2176, 2019.

[29] J. J. Otto and R. D. Campbell, “Tissue economics of hydra: regulation of cell cycle, animal size and development by controlled feeding rates,” *J. Cell Sci.*, vol. 28, no. 1, pp. 117 LP – 132, Dec. 1977.

[30] H. Bode, S. Berking, C. N. David, A. Gierer, H. Schaller, and E. Trenkner, “Quantitative analysis of cell types during growth and morphogenesis in Hydra,” *Wilhelm Roux. Arch. Entwickl. Mech. Org.*, vol. 171, no. 4, pp. 269–285, 1973.

[31] K. N. Badhiwala, D. L. Gonzales, D. G. Vercosa, B. W. Avants, and J. T. Robinson, “Microfluidics for electrophysiology, imaging, and behavioral analysis of: Hydra,” *Lab Chip*, vol. 18, no. 17, pp. 2523–2539, 2018.

[32] G. Duret *et al.*, “Magnetic Entropy as a Proposed Gating Mechanism for Magnetogenetic Ion Channels,” *Biophys. J.*, vol. 116, no. 3, pp. 454–468, Feb. 2019.